Available online at www.sciencedirect.com
SCIENCE DIRECT
Physics of the Earth and Planetary Interiors 155 (2006) 96–103
PHYSICS OF THE EARTH AND PLANETARY INTERIORS
www.elsevier.com/locate/pepi

Al, Fe substitution in the $MgSiO_3$ perovskite structure: A single-crystal X-ray diffraction study

C.B. Vanpeteghem [a,*], R.J. Angel [a], N.L. Ross [a], S.D. Jacobsen [b], D.P Dobson [c], K.D. Litasov [d], E. Ohtani [d]

[a] *Crystallography Laboratory, Department of Geosciences, Virginia Polytechnic Institute and State University, Derring Hall, Blacksburg, VA 24061, USA*
[b] *Geophysical Laboratory, Carnegie Institute of Washington, 5251 Broad Branch Road, NW, Washington DC 20015, USA*
[c] *Department of Earth Sciences, University College London, Gower Street, London WC1E 6BT, UK*
[d] *Institute of Mineralogy, Petrology and Economic Geology, Tohoku University, Sendai 981-8578, Japan*

Received 22 April 2005; received in revised form 22 August 2005; accepted 12 October 2005

Abstract

We have determined by single-crystal X-ray diffraction the crystal structure of three Fe–Al–$MgSiO_3$ perovksite samples containing up to 9.5 wt% of Al_2O_3 and 19 wt% of FeO. We find that there is no evidence for Fe (Fe^{3+} or Fe^{2+}) on the octahedral site. Therefore, we deduce that the two dominant substitution mechanisms for the combined substitution of Al and Fe into the perovskite structure are: (i) $Mg_A{}^{2+} + Si_B{}^{4+} \Leftrightarrow Fe_A{}^{3+} + Al_B{}^{3+}$, where the excess of Fe is accommodated by (ii) $Mg_A{}^{2+} \Leftrightarrow Fe_A{}^{2+}$. This is in agreement with all past theoretical and experimental work and solves the long-debated issue of Fe^{3+} occupancy in the perovskite structure.

Keywords: Single-crystal; X-ray diffraction; Cation partitioning; Site occupancy

1. Introduction

Magnesium silicate perovskite ($MgSiO_3$) is believed to be the dominant phase in Earth's lower mantle, coexisting with magnesiowüstite (Mg,Fe)O and $CaSiO_3$ perovskite (e.g. Kesson et al., 1998; Serghiou et al., 1998; Shim et al., 2004). The physical and chemical properties of perovskite and magnesiowüstite, and the distribution of major elements between these phases should therefore account for the bulk seismic properties of the lower mantle. In particular, partitioning of iron (Fe^{2+} and Fe^{3+}) and aluminum between the various phases is expected to influence the elasticity and rheology of the lower mantle (e.g. Jackson, 1998; Kung et al., 2002; Yamazaki and Karato, 2002), its bulk transport properties (e.g. Xu et al., 1998) as well as possible compositional layering (e.g. Kellogg et al., 1999; Badro et al., 2003). Since cation partitioning is ultimately controlled by structure, a detailed picture of silicate perovskite crystal chemistry with varying Fe and Al substitution is necessary to further our understanding of the lower mantle assemblage.

Over the past 10 years, much effort has been made to determine the effect of Al substitution on the physiochemical properties of Fe–$MgSiO_3$ perovskite (e.g. McCammon, 1997; Richmond and Brodholt, 1998; Wood, 2000; Brodholt, 2000; Lauterbach et al., 2000; Andrault et al., 2001). Previous work by Wood and

* Corresponding author. Tel.: +1 540 231 5539; fax: +1 540 231 3386.
E-mail address: carine@vt.edu (C.B. Vanpeteghem).

0031-9201/$ – see front matter © 2005 Elsevier B.V. All rights reserved.
doi:10.1016/j.pepi.2005.10.003

Rubie (1996) and Frost and Langenhorst (2002) indicated that the presence of Al causes a significant increase in the partioning of Fe into Fe–$MgSiO_3$ perovskite coexisting with magnesiowütstite. It is, therefore, of critical importance to determine site occupancies of all possible cations that could be hosted by magnesium silicate perovskite.

The perovskite structure, generally ABO_3, is composed of a corner-linked octahedral framework (B cation site) with the octahedra sharing triangular faces with a larger dodecahedral A cation site formed by the spaces within the three-dimensional octahedral network. The structure of Al–Fe–$MgSiO_3$ perovskite (space group *Pbnm*) is an orthorhombic distortion from the ideal cubic perovskite structure with space group *Pm*3*m* (Horiuchi et al., 1987).

Previous studies (Horiuchi et al., 1987; Kudoh et al., 1990; McCammon et al., 1992; Fei et al., 1994; McCammon, 1998; Jackson et al., 2005) determined that Fe on its own substitutes into $MgSiO_3$ by the following exchange mechanisms:

$$Mg_A{}^{2+} + Si_B{}^{4+} \Leftrightarrow Fe_A{}^{3+} + Fe_B{}^{3+} \quad (1)$$

$$Mg_A{}^{2+} \Leftrightarrow Fe_A{}^{2+} \quad (2)$$

where the subscripts A and B refer to the dodecahedral A-site and octahedral B-site, respectively. McCammon (1998) reported that in the presence of oxygen vacancies, Fe^{3+} is located on the octahedral site but as the concentration of Fe^{3+} increases in phases synthesized at higher oxygen fugacity, Fe^{3+} occupies both sites. Lauterbach et al. (2000) showed that an additional substitution mechanism can operate along with mechanisms (1) and (2) through creation of oxygen vacancies when Fe^{3+} replaces Si^{4+} as follows: $\frac{1}{2}O_2{}^- + Si_B{}^{4+} \Leftrightarrow \frac{1}{2}V_o + Fe_B{}^{3+}$. This mechanism is analogous to that described for Fe substitution in $CaTiO_3$ (Becerro et al., 1999).

In Fe-free $MgSiO_3$, Al substitution is accommodated by two mechanisms analogous to those found for Fe substitution (Kesson et al., 1995; Andrault et al., 1998; Stebbins et al., 2001, 2003; Yamamoto et al., 2003; Navrotsky et al., 2003; Akber-Knutson and Bukowinski, 2004):

$$Mg_A{}^{2+} + Si_B{}^{4+} \Leftrightarrow Al_A{}^{3+} + Al_B{}^{3+} \quad (3)$$

$$\frac{1}{2}O_2{}^- + Si_B{}^{4+} \Leftrightarrow \frac{1}{2}V_o + Al_B{}^{3+} \quad (4)$$

The vacancy substitution mechanism (4) is suppressed by increasing pressure and is only significant in the uppermost part of the lower mantle (Brodholt, 2000).

In addition, numerous previous synthesis and phase-equilibrium studies of Al incorporation into Fe–$MgSiO_3$ (e.g. Wood and Rubie, 1996; McCammon, 1997; Richmond and Brodholt, 1998; Wood, 2000; Brodholt, 2000; Lauterbach et al., 2000; Andrault et al., 2001; Frost and Langenhorst, 2002) have shown that (i) the Fe^{3+} content of $MgSiO_3$ perovskite increases with Al content and is independent of oxygen fugacity, (ii) Fe^{2+} partitioning is independent of Al_2O_3 content and (iii) the substitution of 3+ cations is coupled with Al substitution, where the highest level of cations are for X = Fe, Sc, Ga and Y (Andrault et al., 2001; Andrault, 2003).

In summary, previous studies indicate that Fe^{2+} occupies the dodecahedral A-site, whereas the location of Fe^{3+} within the silicate perovskite structure remains unclear. Therefore, we have carried out a single-crystal X-ray diffraction study on several well-characterized Fe–Al–$MgSiO_3$ crystals to determine the site occupancies of Al and Fe, and hence deduce the possible substitution mechanisms. Our results, based on the three samples studied here, are in agreement with all previous experimental and theoretical work and solve the question of Fe^{3+} occupancy in the lower mantle perovskite structure.

2. Experimental methods

Five different synthetic samples of Mg-perovskites have been used in this study and their compositions are summarized in Table 1. The Mg-perovskites were synthesized at 24–25 GPa and 1750–2000 °C in a multi-anvil press apparatus available at the Bayerisches Geoinstitut by Bolfan-Casanova (2000) and Dobson and Jacobsen (2004). Al and Fe-bearing samples were synthesized by Dobson and Jacobsen (2004) at the Bayerisches Geoinstitut and by Litasov and Ohtani (2002) in a Kawai-type (MA8) multi-anvil press at Tohoku University (Litasov and Ohtani, 2002). Bolfan-Casanova (2000) used oxide mixtures of MgO, SiO_2 and $Mg(OH)_2$ as a starting material. The temperature was held at ~1750 °C for up to 10 h before rapid quenching and slow decompression lasting 12–30 h. Chemical analyses were performed with a Cameca SX50 electron microprobe at 15 nA and 15 kV.

Dobson and Jacobsen (2004) synthesized large pure-Mg and Al–Fe–Mg-perovskite crystals up to 300 μm in size by fluxing the system in molten NaCl at 24 GPa. Temperature cycling between 1850 and 2050 °C was used to enhance grain growth, before rapid quenching and ~15 h decompression. The chemical compositions of the samples were determined using a JEOL 733 electron microscope on as-grown (not polished) crystals at 2 nA and 15 kV.

Two additional samples of Al–Fe–Mg-perovskite, one corresponding to peridotite and the other having closer to MORB composition, were synthesized from

Table 1
Chemical composition of the silicate perovskite samples

Sample #	1 $MgSiO_3$[a]	2 $MgSiO_3$[b]	3 $MgAlFeSiO_3$[b]	4 $MgAlFeSiO_3$[c]	5 $MgAlFeSiO_3$[c]
NaO_2	–	0.24(2)	0.53(3)	–	–
MgO	∼37[d]	40.3(8)	37.1(7)	34.4(2)	25.5(8)
Al_2O_3	–	–	1.00(4)	5.6(4)	9.5(7)
SiO_2	∼60[d]	59.4(7)	58.6(4)	53.2(3)	44(1)
FeO	–	–	2.8(3)	6.1(4)	19(1)
TiO_2	–	–	–	–	2.2(3)
Na	–	0.008	0.017	–	–
Mg	0.958	1.002	0.934	0.883	0.686
Al	–	–	0.020	0.113	0.202
Fe	–	–	0.040	0.088	0.287
Si	1.042	0.990	0.989	0.916	0.795
Ti	–	–	–	–	0.030

[a] Bolfan-Casanova (2000).
[b] Dobson and Jacobsen (2004).
[c] This work.
[d] The sample contains a small amount of Cr.

mixed oxide starting materials (plus variable amounts of water added as brucite) by Litasov et al. (2003). For the peridotite-type Mg-perovskite, an oxide mixture was used as a starting material. 10 wt% H_2O as $Mg(OH)_2$ was added to the sample, with an appropriate adjustment of the proportion of MgO to maintain the perovskite stoichiometry. The sample was synthesized at 25 GPa and 1800 °C for up to 6 h before rapid quenching. FTiR measurements on the recovered sample show no evidence for water. In the MORB sample, minor stishovite and quenched melt were observed in recovered samples. The sample was synthesized at 25 GPa and 1250 °C for 6 h. Once again, no water was detected in the synthesized sample. In the peridotite sample, the perovskite coexisted with majorite-garnet, because the synthesis temperature was below that of perovskite-magnesiowüstite stability. The chemical composition of the Al–Fe–Mg-perovskites was determined by electron microprobe (JEOL Superbrobe, JXA-8800) under the operating conditions of 15 kV and 10 nA specimen current.

All perovskite samples showed broadened diffraction peak profiles when examined by a point detector, which we attribute mostly to cracking and development of sub-grain boundaries, probably on decompression in the multi-anvil press. Subsequent analysis also indicates the presence of minor twinning on {1 1 0} in some samples. We therefore used an Xcalibur-2 diffractometer equipped with a Sapphire-III CCD detector for intensity data collection, which allows the entire peak profile at each peak to be integrated directly on to the detector. Absorption corrections were performed by numerical integration in ABSORB 6.0 (Angel, 2004). After averaging the symmetrically equivalent reflections, the remaining independent reflections with ($F > 4\sigma$ (F)) were used to refine structures with RFINE99, an updated version of RFINE4 (Finger and Price, 1974).

The potential for several different cations to occupy both the A and B cation sites of these perovskites, together with the possibility of vacancies on the anion positions, means that refinement models have to be constructed and interpreted with care so as to not bias the results. First, we note that the X-ray scattering factors of Al, Si and Mg atoms are very similar so they cannot be distinguished by direct refinement of site occupancies. We therefore used the scattering factor for Si to represent the total occupancy of Mg + Al + Si on the B-site, and the scattering factor of Mg to represent the total occupancy of Mg + Al + Si on the A-site. However Fe, with approximately twice the scattering power than Al, Si and Mg, can be readily distinguished by X-ray diffraction measurements. Since the ionic scattering factors of Fe^{2+} and Fe^{3+} are very similar, we used the scattering factors of neutral atoms in all refinements. The cation site occupancies were then refined as Mg + Fe for the A-site, and Si + Fe for the B-site, with the assumption that both sites are 100% occupied. When the refined Fe content of a site fell to zero it was fixed at zero in the final refinements reported here.

Given the nature of X-ray diffraction measurements, it is not possible to simultaneously refine the occupancies of all of the atomic sites within a crystal structure. It is therefore not possible to simultaneously refine the cation site occupancies and the vacancy content of the oxygen sites in these perovskites. Therefore, for each refinement

Table 2
Unit cell parameters, refinement parameters, refined fractional occupancies, refined atomic coordinates and equivalent isotopic temperature factor (B_{eq}) of $MgSiO_3$ and $(Mg,Fe)(Al,Si)O_3$

Sample #	1 $MgSiO_3$[a]	2 $MgSiO_3$[b]	3 $MgFeAlSiO_3$[b]	4 $MgFeAlSiO_3$[c]	5 $MgFeAlSiO_3$[c]
Cell parameters					
a (Å)	4.7803(9)	4.7780(2)	4.809(1)	4.7820(1)	4.8078(3)
b (Å)	4.9265(8)	4.9298(3)	4.924(1)	4.9422(2)	5.0066(2)
c (Å)	6.8974(1)	6.8990(3)	6.918(1)	6.9207(3)	7.0358(1)
V (Å^3)	162.43(3)	162.502(1)	163.814(1)	163.561(1)	169.357(1)
Nb. reflections	3145	1511	2366	1242	2753
Density	4.138	4.106	4.106	4.188	4.301
R_{int}	0.030	0.06	0.025	0.021	0.031
Refinement					
Nb. reflections	422	372	219	211	179
R_u	0.028	0.024	0.035	0.021	0.018
R_w	0.035	0.064	0.036	0.020	0.015
Mg, Fe, Al (A-site)					
X_{Mg}	1.00	1.00	0.927(2)	0.931(1)	0.719(5)
X_{Fe}	–	–	0.028	0.069	0.281
x	0.5139(2)	0.5138(1)	0.5128(4)	0.5136(2)	0.5164(2)
y	0.5558(2)	0.5559(1)	0.5550(3)	0.5564(2)	0.5608(1)
z	0.25	0.25	0.25	0.25	0.25
B_{eq}	0.46(1)	0.83(2)	0.83(4)	0.59(2)	0.60(2)
Si, Al (B-site)					
X_{Si} or X_{Al+Si}	1.00	1.00	1.00	1.00	1.00
x	0.50	0.50	0.50	0.50	0.50
y	0.00	0.00	0.00	0.00	0.00
z	0.50	0.50	0.50	0.50	0.50
B_{eq}	0.25(1)	0.58(1)	0.65(3)	0.48(2)	0.59(2)
O_1					
x	0.1032(4)	0.1019(3)	0.1019(8)	0.1063(5)	0.1155(5)
y	0.4664(4)	0.4664(2)	0.4650(6)	0.4635(4)	0.4551(4)
z	0.25	0.25	0.25	0.25	0.25
B_{eq}	0.33(2)	0.73(2)	0.82(6)	0.63(4)	1.01(5)
O_2					
x	0.1968(3)	0.1963(2)	0.1959(4)	0.1951(2)	0.1922(3)
y	0.2013(3)	0.2013(2)	0.2007(4)	0.1993(3)	0.1965(3)
z	0.5524(2)	0.5526(1)	0.5529(4)	0.5524(2)	0.5592(2)
B_{eq}	0.33(2)	0.75(2)	0.83(4)	0.61(3)	1.11(4)

[a] Bolfan-Casanova (2000).
[b] Dobson and Jacobsen (2004).
[c] This work.

we fixed the oxygen vacancy content at a chosen value and then refined the cation site occupancies. As expected, the refined Fe content changes with the chosen oxygen vacancy level, and comparison with the compositions determined by microprobe analysis provides a test of the validity of each vacancy model. A further test is provided by the resulting quality of fit to the measured intensity data, which changes significantly with oxygen vacancy content.

Our refinement models also take into account the presence of a minor twin component in two of our samples, by refining the data with the appropriate twin law. Finally, all refinements include anisotropic displacement parameters. Details of the refinement results are given in Table 2.

3. Results

By using the two pure-Mg perovskite samples as a reference, it is possible to determine how the perovskite structure responds to increasing Al and Fe content. There is a positive volume change with increasing Al and Fe

Table 3
Refined A—O bond lengths (Å) in silicate perovskite

Sample #	1 $MgSiO_3$[a]	2 $MgSiO_3$[b]	3 $MgFeAlSiO_3$[b]	4 $MgFeAlSiO_3$[c]	5 $MgFeAlSiO_3$[c]
A—O_1	2.012(3)	2.017(1)	2.024(4)	1.999(2)	1.998(2)
A—O_2 (×2)	2.056(1)	2.055(1)	2.054(2)	2.046(1)	2.043(2)
A—O_1	2.099(2)	2.098(1)	2.093(3)	2.092(2)	2.074(2)
A—O_2 (×2)	2.281(1)	2.282(1)	2.296(3)	2.286(1)	2.289(1)
A—O_2 (×2)	2.424(1)	2.425(1)	2.431(3)	2.436(1)	2.490(2)
⟨A—O⟩ 8	2.204(2)	2.205(1)	2.209(3)	2.204(2)	2.212(2)
A—O_1	2.851(2)	2.844(1)	2.869(4)	2.873(2)	2.929(2)
A—O_1	2.957(2)	2.957(1)	2.957(3)	2.986(2)	3.098(2)
A—O_2 (×2)	3.115(1)	3.117(1)	3.123(2)	3.142(1)	3.237(1)
⟨A—O⟩ 12	2.472(2)	2.473(1)	2.479(3)	2.481(2)	2.516(2)

[a] Bolfan-Casanova (2000).
[b] Dobson and Jacobsen (2004).
[c] This work.

content. As the amount of Al increases from 0 to 2%, 11.3 and 20.7% along with Fe from 0 to 4%, 8.8 and 28.5%, the volume increases, respectively, by 0.8, 0.7 and 4.2% resulting in density increases of 1.5 and 4.5% for the most Fe-rich samples. The unit cell volume increase due to Al and Fe has been observed in previous work (e.g. Andrault et al., 2001).

In all of the structure refinements the Fe content of the B-site refined to zero. Test refinements with 1 mol% of Fe (2 mol% for sample #3) allocated to the B-site result in a significant decrease in the quality of fit to the measured intensity data as indicated by an increase in the *R*-values. Therefore, the possibility of more than 2 mol% of Fe occupying the B-site can be excluded, and all subsequent refinements were performed with the Fe content of the B-site fixed at zero. Consequently, all the Fe atoms occupy the A-site of the perovskite structure. For the three perovskite samples containing 4, 8.8 and 28.5% of Fe as determined by EPMA analysis, we found that the Fe fractional occupancies on the A-site are, respectively, 2.8, 6.9 and 28.1%, the slight discrepancies in the numbers lying within the combined experimental uncertainties of the refinement and the chemical analysis.

Since X-ray diffraction allows only the measurement of the relative scattering power of each site, we observe, as expected, a decrease in the refined Fe content when the fixed oxygen vacancy content is increased. Adding oxygen vacancies therefore leads to a mismatch between the iron content and the chemical composition. For sample #3, starting with 2.8% of Fe, adding 1–5% of oxygen vacancies in the structure reduced the refined Fe content from 2.6 to 2% (in this case, 1% of oxygen vacancies is not excluded but not favored). Similarly, for samples #4 and #5, respectively, starting with 6.9 and 28%, the addition of 1–5% of oxygen vacancies gives 6.5–5.2% of Fe and 26.9–22% of Fe. In addition, if we fix the fractional occupancy of Fe as measured by the chemical composition and as given by our best refinement, the final *R*-value significantly increases with the amount of oxygen vacancies. It is therefore clear from our results that the best description of the perovskite structures is the one without oxygen vacancies, as presented in Tables 1–5. This is in agreement with computer simulations, which show that at the high pressure and temperature conditions under which the samples were synthesized, the amount of energy required to create oxygen vacancies would be very high (Richmond and Brodholt, 1998).

Examination of the structural parameters in Tables 3–5 shows that the addition of Fe + Al into the perovskite structure results in (i) an increase of the average ⟨A–O⟩ bond distances, (ii) a shortening of the three shortest A–O bonds and (iii) an expansion of the nine longer A–O distances (Fig. 1 and Table 3). This is a consequence of the increased tilting of the BO_6 octahedra that is also clearly indicated by the decrease of the B—O—B angles (Fig. 2 and Table 5). Consequently, the structure gets more distorted as Al and Fe are added into the structure. Internally to the octahedra, the O—B—O angles do not change significantly with composition but the average bond lengths ⟨B—O⟩ increase with Al and Fe content (Table 4). Since the refinements indicate that no significant amount of Fe occupies the B-site, we deduce that the B-site expansion must be due to an increase of Al occupancy on the B-site; pure aluminate perovskites have average ⟨B—O⟩ bond lengths in the range of 1.899–1.910 Å.

Table 4
Refined B—O bond lengths (Å) in silicate perovskite

Sample #	1 $MgSiO_3$[a]	2 $MgSiO_3$[b]	3 $MgFeAlSiO_3$[b]	4 $MgFeAlSiO_3$[c]	5 $MgFeAlSiO_3$[c]
B—O_1 (×2)	1.8011(6)	1.7829(8)	1.806(1)	1.8126(7)	1.858(1)
B—O_2 (×2)	1.793(1)	1.7998(4)	1.803(2)	1.799(1)	1.826(2)
B—O_2 (×2)	1.784(1)	1.7952(8)	1.787(2)	1.794(1)	1.825(1)
⟨B—O⟩	1.793(3)	1.793(7)	1.799(2)	1.802(3)	1.836(1)

[a] Bolfan-Casanova (2000).
[b] Dobson and Jacobsen (2004).
[c] This work.

Table 5
Interatomic angles within the B-site and B—O—B angles (degrees)

Sample #	1 $MgSiO_3$[a]	2 $MgSiO_3$[b]	3 $MgFeAlSiO_3$[b]	4 $MgFeAlSiO_3$[c]	5 $MgFeAlSiO_3$[c]
O_1—B—O_2	88.72(7)	88.48(3)	88.5(1)	88.48(8)	88.1(1)
O_1—B—O_2	91.49(7)	91.20(6)	91.5(1)	91.61(8)	91.9(1)
O_2—B—O_2	89.37(2)	89.30(6)	89.02(4)	89.32(3)	89.07(4)
O_2—B—O_2	90.63(2)	90.71(5)	90.98(4)	90.68(3)	90.93(4)
B—O_1—B	146.4(1)	146.4(3)	146.5(2)	145.3(1)	142.0(2)
B—O_2—B	147.32(8)	147.3(2)	147.0(1)	146.17(9)	143.3(1)

[a] Bolfan-Casanova (2000).
[b] Dobson and Jacobsen (2004).
[c] This work.

4. Discussion

The refinement results indicate that there are little or no oxygen vacancies in these perosvkites, and 1 mol% or less of Fe on the B cation sites within the structures. In combination with the measured chemical compositions, these results indicate that not only does effectively all of the Fe reside on the A cation site, but that all of the Al resides on the B cation site, as indicated by the measured increase in B—O bond lengths. These site occupancies are consistent with the results of Mössbauer and ELNES spectroscopy measurements of similar samples (Lauterbach et al., 2000). A consequence of our observations is that the following substitution mechanisms dominate in Al–Fe–$MgSiO_3$ perovskites in which the Fe content exceeds the Al content:

$$Mg_A{}^{2+} + Si_B{}^{4+} \Leftrightarrow Fe_A{}^{3+} + Al_B{}^{3+} \quad (5)$$

$$Mg_A{}^{2+} \Leftrightarrow Fe_A{}^{2+} \quad (6)$$

These substitution mechanisms correspond to a solid solution between $MgSiO_3$ and the end-member components $Fe^{3+}Al^{3+}O_3$ and $FeSiO_3$. They can be easily understood in terms of the known substitution mechanisms of Fe into $MgSiO_3$ and Al into $MgSiO_3$ as described in Section 1 and by considering the effect of Al substitution into Fe–$MgSiO_3$.

The coupled substitution represented by Eq. (5) is a combination of those given in Eqs. (1) and (3), with Fe substituting for Mg on the A-site and Al^{3+} for the Si^{4+} on the B-site (though some amount of Al on the A-site cannot be excluded on the basis of X-ray diffraction alone) and the excess of Fe is accounted by Eq. (2). This agrees with density functional theory calculations (Brodholt, 2000), which show that the substitution of Fe onto the A-site and Al^{3+} onto the B-site is enegetically favored over the opposite situation in which Fe^{3+} would occupy the B-site and Al^{3+} the A-site. This coupled substitution of Fe and Al Eq. (5) also explains the observation that the substitution of other trivalent cations is strongly coupled to Al content (Andrault, 2003). In our samples, the excess of Fe over Al is accommodated by mechanism (6), which is also found in Al-free $MgSiO_3$ (e.g. Kudoh et al., 1990; Kesson et al., 1995; McCammon, 1998; Jackson et al., 2005). Further, our structure determination shows that there is no significant substitution involving oxygen vacancies, in agreement with previous theoretical calculations (Brodholt, 2000).

In summary, our results demonstrate that the incorporation of Al and Fe into the end-member $MgSiO_3$

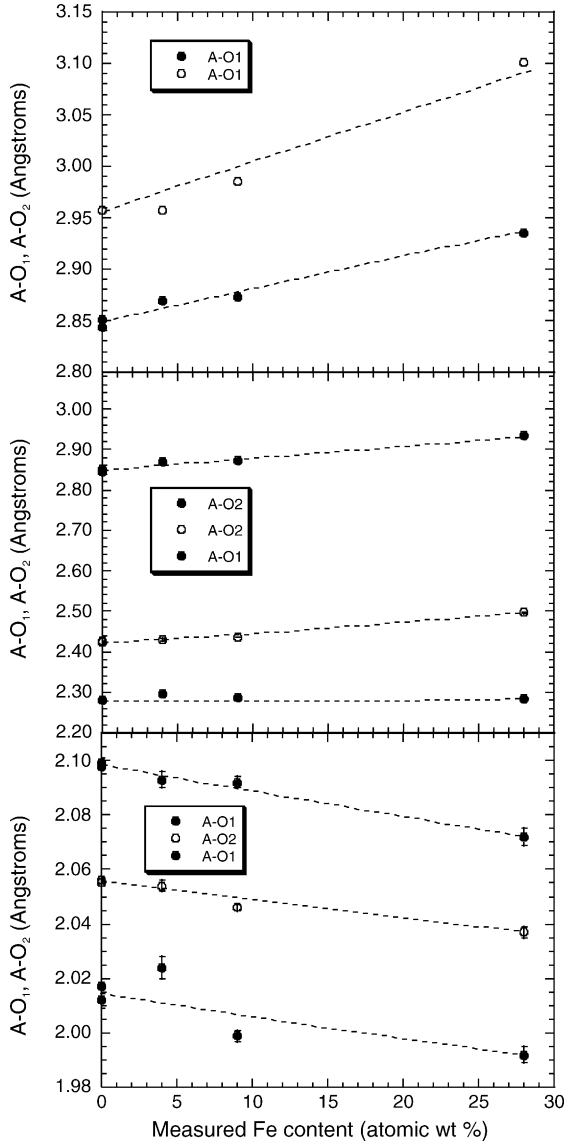

Fig. 1. Variation of the A—O bond lengths with Fe-content for silicate perovskite. The dotted line is used as a guideline to the eye. The shortest bond lengths get shorter while the longest bonds get longer as the Fe content increases.

perovskite occurs via mechanism represented by Eqs. (5) and (6). We can rule out the formation of oxygen vacancies and the incorporation of any Fe on the B-site. This is true for all three samples studied here, and especially for the sample in which the Fe content exceeded by far that of samples characterized in numerous earlier studies. We conclude from our results that the effect of Al is to drive all Fe onto the A-site. The question remains as to how the incorporation of Fe and Al changes the structure of Al–Fe–$MgSiO_3$ at the pressure and temperature conditions of the lower

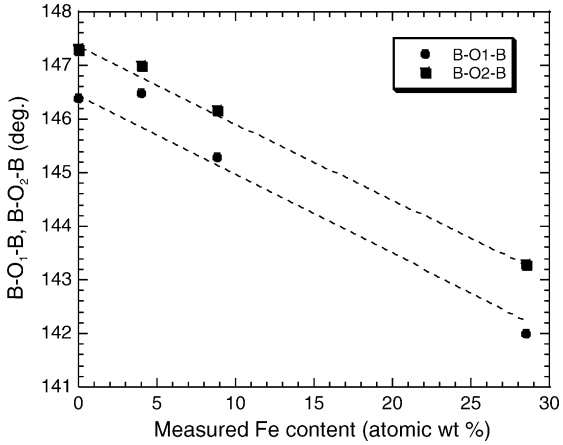

Fig. 2. Variation of the distortion angle B—O—B with Fe content in silicate perovskite. As the Fe content increases, the angle decreases making the structure more distorted. The estimated uncertainties are the size of the symbols.

mantle and influences the chemistry of the deep Earth's mantle.

Acknowledgments

This work is supported by NSF-EAR 0105864 and EAR 0408460 awarded to Nancy L. Ross and Ross J. Angel and NSF-CHE 0131128 to Carla Slebodnick. C.B. Vanpeteghem acknowledges financial support from the Advance VT-SPE 0244916 Fellowship. Steve Jacobsen is supported by NSF-EAR-0440112 and by a Carnegie Fellowship. This work is also supported by the Grant-in-aid of Scientific Research of Priority Area (no. 16075202) from Monbusho to Eiji Ohtani.

References

Akber-Knutson, S., Bukowinski, M.S.T., 2004. The energetics of aluminum solubility into $MgSiO_3$ perovskite at lower mantle conditions. Earth Sci. Planet. Lett. 7014, 1–14.

Andrault, D., 2003. Cation substitution in $MgSiO_3$ perovskite. Phys. Earth Planet. Inter. 136, 67–78.

Andrault, D., Bolfan-Casanova, N., Guignot, N., 2001. Equations of state of lower mantle (Al, Fe)-$MgSiO_3$ perovskite. Earth Planet. Sci. Lett. 193, 501–508.

Andrault, D., Neuville, D.R., Flanck, A.-M., Wang, Y., 1998. Cation sites in Al-rich $MgSiO_3$ perovskites. Am. Miner. 83, 1045–1053.

Angel, R.J., 2004. Absorption corrections for diamond-anvil cell implemented in the software package Absorb 6.0. J. Appl. Cryst. 37, 486–492.

Badro, J., Fiquet, G., Guyot, F., Rueff, J.P., Struzhkin, V.V., Vanko, G., Monaco, G., 2003. Iron partitioning in Earth's mantle: toward a deep lower mantle discontinuity. Science 300, 789–791.

Becerro, A.I., McCammon, C.A., Langenhorst, F., Seifert, F., Angel, R.J., 1999. Oxygen vacancy ordering in $CaTiO_3$-$CaFeO_{2.5}$ per-

ovskites: from isolated defects to infinite sheets. Phase Trans. 69, 133–146.

Bolfan-Casanova, 2000. Ph.D. thesis.

Brodholt, J.P., 2000. Pressure-induced changes in the compression mechanism of aluminous perovskite in the Earth's lower mantle. Nature 407, 620–622.

Dobson, D.P., Jacobsen, S.D., 2004. The flux growth of magnesium silicate perovskite single crystals. Am. Miner. 89, 807–811.

Fei, Y., Virgo, D., Mysen, B.O., Wang, Y., Mao, H.K., 1994. Temperature dependent electron delocalization in (Mg,Fe)SiO_3 perovskite. Am. Miner. 79, 826–837.

Finger, L.W., Price, E., 1974. US Nat Bur. Stand, NBS, Tech note, 854-xxx, Washington DC.

Frost, D.J., Langenhorst, F., 2002. The effect of Al_2O_3 on Fe–Mg partitioning between magnesiowüstite and magnesium silicate perovskite. Earth Planet. Sci. Lett. 199, 227–241.

Horiuchi, H., Ito, E., Weidner, D.J., 1987. Perovskite-type $MgSiO_3$: single-crystal X-ray diffraction study. Am. Miner. 72, 357–360.

Jackson, I., 1998. Elasticity, composition and temperature of the Earth's lower mantle: a reappraisal. Geophys. J. Int. 134, 291–311.

Jackson, J.M., Sturham, W., Stem, G., Zhao, J., Hu, M.Y., Errandonea, D., Bass, J.D., Fei, Y., 2005. A synchrotron Mössbauer spectroscopy study of (Mg,Fe)SiO_3 perovskite up to 120 GPa. Am. Miner. 90, 199–205.

Kellogg, L.H., Hager, B.H., van der Hilst, R.D., 1999. Compositional stratification in the deep mantle. Science 283, 1881–1884.

Kesson, S.E., Fitz Gerald, J.D., Shelley, J.M.G., 1998. Mineralogy and dynamics of a pyrolite lower mantle. Nature 393, 252–255.

Kesson, S.E., Fitz Gerald, J.D., Shelley, J.M., Withers, R.L., 1995. Phase relations, structure and crystal chemistry of some aluminous silicate perovskites. Earth Planet. Sci. Lett. 134, 187–201.

Kudoh, Y., Prewitt, C.T., Finger, L.W., Daravskikh, A., Ito, E., 1990. Effect of Fe on the crystal structure of (Mg, Fe)SiO_3 perovskite. Geophys. Res. Lett. 17 (10), 1481–1484.

Kung, J., Li, B., Weidner, D.J., Zhang, J., Liebermann, R.C., 2002. Elasticity of ($Mg_{0.83}Fe_{0.17}$)O ferropericlase at high pressure: ultrasonic measurements in conjunction with X-radiation techniques. Earth Planet. Sci. Lett. 203, 557–566.

Lauterbach, S., McCammon, C.A., van Aken, P., Langenhorst, F., Seifert, F., 2000. Mössbauer and ELNES spectroscopy of (Mg,Fe)(Si,Al)O_3 perovskite: a highly oxidized component of the lower mantle. Contrib. Mineral. Petrol. 138, 17–26.

Litasov, K.D., Ohtani, E., 2002. Phase relations and melt compositions in CMAS pyrolite-H_2O system up to 25 GPa. Phys. Earth Planet. Inter. 134, 105–127.

Litasov, K.D., Ohtani, E., Langenhorst, F., Yurimoto, H., Kubo, T., Kondo, T., 2003. Water solubility in Mg-perovskites and water storage capacity in the lower mantle. Earth Planet. Sci. Lett. 211, 189–203.

McCammon, C.A., 1997. Perovskite as a possible sink for ferric iron in the lower mantle. Nature 387, 694–696.

McCammon, C.A., 1998. The crystal chemistry of ferric iron in $Fe_{0.05}Mg_{0.95}SiO_3$ perovksite as determined by Mössbauer spectroscopy in temperature range 80–293 K. Phys. Chem. Miner. 25, 292–300.

McCammon, C.A., Rubie, D.C., Ross II., C.R., Seifert, S., O'Neill, H.S.C., 1992. Mössbauer spectra of $^{57}Fe_{0.05}Mg_{0.95}SiO_3$ perovskite at 80 K and 298 K. Am. Miner. 77, 894–897.

Navrotsky, A., Schoenitz, M., Kojitani, H., Xu, H., Zhang, J., Weidner, D.T., Jeanloz, R., 2003. Aluminum in magnesium silicate perovskite: formation, structure and energetics of Mg-rich defect solid solutions. J. Geophys. Res. 108, 2330, doi:10.1029/2002JB002055.

Richmond, N.C., Brodholt, J.P., 1998. Calculated role of aluminum in the incorporation of ferric iron into magnesium silicate perovskite. Am. Miner. 83, 947–951.

Shim, S.-H., Duffy, T.S., Jeanloz, R., Shen, G., 2004. Stability and crystal structure of $MgSiO_3$ perovskite to the core-mantle boundary. Geophys. Res. Lett. 31, L10603, doi:10.1029/2004GL019639.

Serghiou, G., Zerr, A., Boehler, R., 1998. (Mg,Fe)-SiO_3-perovksite stability under lower mantle conditions. Science 280, 2093–2095.

Stebbins, J.F., Kojitani, H., Akaogi, M., Navrotsky, A., 2003. Aluminum substitution in $MgSiO_3$ perovskite: investigation of multiple mechanisms by ^{27}Al NMR. Am. Miner. 88, 1161–1164.

Stebbins, J.F., Krocker, S., Andrault, D., 2001. The mechanism of solution of Al oxide in $MgSiO_3$ perovskite. Geophys. Res. Lett. 28, 615–618.

Wood, B.J., Rubie, D.C., 1996. The effect of alumina on phase transformations at the 660-kilometer discontinuity from Fe–Mg partitioning experiments. Science 273, 1522–1524.

Wood, B.J., 2000. Phase transformations and partitioning relations in peridotite under lower mantle conditions. Earth Planet. Sci. Lett. 174, 341–354.

Xu, Y.S., McCammon, C.A., Poe, B.T., 1998. The effect of alumina on the electrical conductivity of silicate perovskite. Science 282, 922–924.

Yamamoto, T., Yuen, D.A., Ebisuzuki, T., 2003. Substitution mechanisms of Al ions in $MgSiO_3$ perovskite under high pressure condtions from first principles calculations. Earth Sci. Planet. Lett. 206, 617–625.

Yamazaki, D., Karato, S., 2002. Fabric development in (Mg,Fe)O during large strain, shear deformation: implications for seismic anisotropy in Earth's lower mantle. Phys. Earth Planet. Inter. 131, 251–267.